

Supplementary Information for “Electrochemistry in a drop: a study of the electrochemical behaviour of mechanically exfoliated graphene on photoresist coated silicon substrate”

Raman characterisation of graphene flakes at different substrates

Raman spectra for different flakes are reported in Fig S1; S1A shows representative spectra of the flakes on Si/SiO₂ substrate after the mechanical exfoliation, while Fig S1B shows the spectra of graphene layers after transferring to Si/SU8 substrate with CAB. Baseline correction was applied for graphene flakes spectra on Si/SU8.

The G band in both cases could be seen at about 1580 cm⁻¹ and the 2D band is present at around 2650 cm⁻¹ and 2710 cm⁻¹ depending from the substrate. On Si/SiO₂, before the transfer (Fig S1A): the change of the 2D band shape and the peak position shift indicate the different number of layers. While on the Si/SU8 substrate (Fig S1B) the distinction for the number of layers is possible only from the shift of the 2D band: 2650 cm⁻¹ in the case of monolayer and for few-layer is 2689 cm⁻¹, such as for the graphite flake.

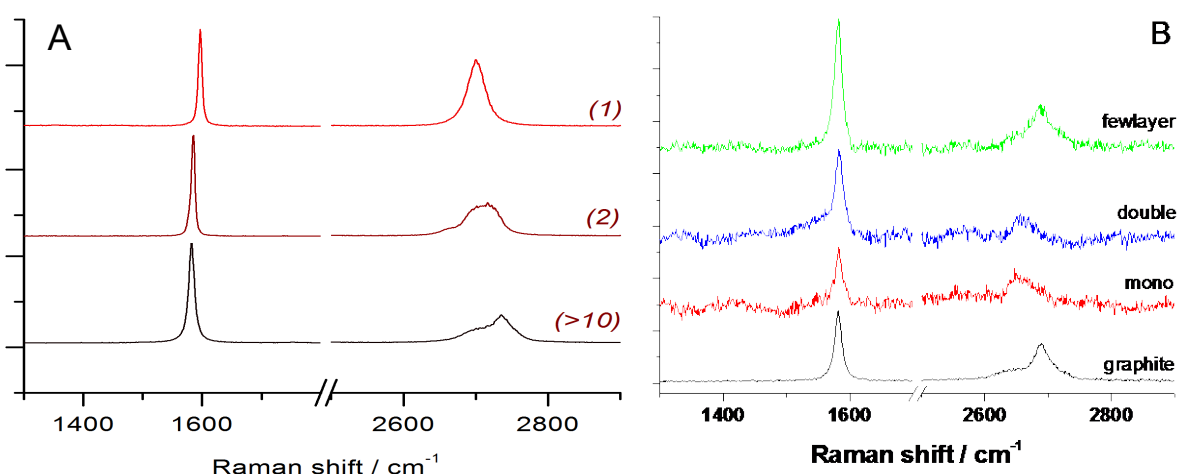


Figure S1. Raman spectra performed at the different graphene layers on Si/SiO₂ (A) and Si/SU8 (B) substrate.

Diffusion coefficient determination

In order to determine the diffusion coefficient of the IrCl₆²⁻ reduction, several cyclic voltammetric and chronoamperometric measurements were performed with Pt disc and microdisc electrodes.

Figure S2 A and B show potentiodynamic and potentiostatic signal on Pt disc electrodes. Figure S2A provides an overview of the voltammetric curves recorded of 5 mM (NH₄)₂IrCl₆ and 6 M LiCl electrolyte at scan rates in the range 50 to 300 mV s⁻¹. The reduction peak current is plotted *versus* the square root of the scan rate in the inset (Fig S2A right) and is consistent with the trend predicted with the Randles-Sevcik equation¹:

$$i_p = 0.4463 \sqrt{\left(\frac{n^3 F^3}{RT}\right)} ACD^{1/2} \nu^{1/2} \quad \text{Eq. 1}$$

where i_p is the reduction peak current; n is the number of electrons transferred in the redox event (1 in the present case); F is the Faraday constant; A is the area of the working electrode; C is the concentration of the electroactive species; D is the diffusion coefficient of the electroactive species (IrCl_6^{2-} in the present case) and ν is the scan rate. The diffusion coefficient calculated from the slope of the linear fitting of the scatter plot in the right inset of Fig S2A, was $2.93 \times 10^{-6} \text{ cm}^2 \text{ s}^{-1}$.

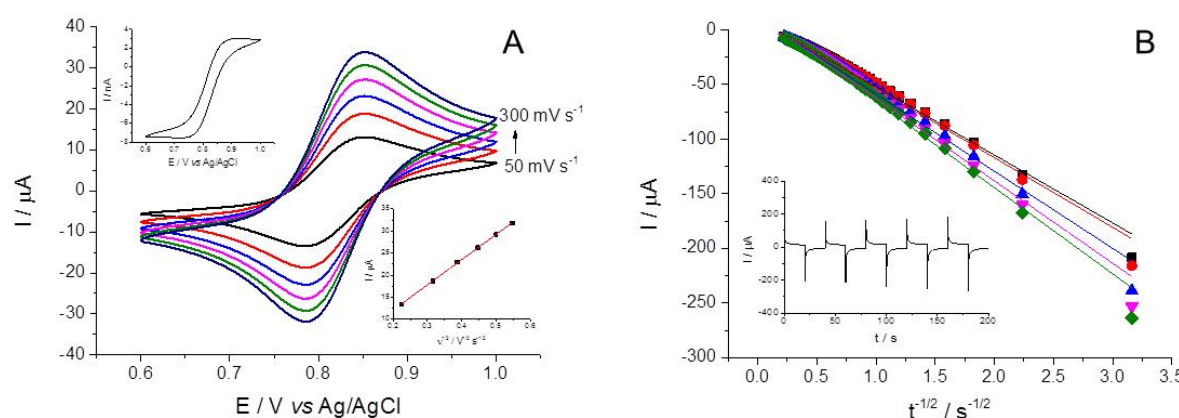


Figure S2. Voltammetric (A) and chronoamperometric (B) responses of 5 mM $(\text{NH}_4)_2\text{IrCl}_6$ and 6 M LiCl electrolyte on 2 mm diameter Pt disc electrode. The magnitude of the reduction peak current is plotted against the square root of scan rate is shown in the right inset of (A). The voltammogram obtained with 25 μm diameter Pt microdisc at 100 mV s^{-1} left inset of (A). Chronoamperometric data were collected by stepping the potential from +1.1 V to -0.5 V 5 times, it shows in inset of (B). The chronoamperometric current is plotted against the reciprocal of square root of time during the five transients (B).

The inset of Fig S2 A (at left) displays the voltammetry signal of IrCl_6^{2-} reduction at 25 μm diameter Pt microdisc electrode. The diffusion limited current (i) for a microdisc electrode is 7.45 nA, according to Eq. 2, where r is the radius of the window to the solution ($r = 12.5 \mu\text{m}$). The calculated D value is $3.09 \times 10^{-6} \text{ cm}^2 \text{ s}^{-1}$.

$$i = 4nFDCr \quad \text{Eq. 2}$$

The current response was recorded for five consecutive potential steps (inset of Fig S2B), each time the potential was stepped from +1.1 V to -0.5 V and held for 20 seconds, on 2 mm diameter Pt disc electrode. Plots of the current against the reciprocal square root of time are shown in Fig S2B. The current response for the droplet is consistent with the Cottrell equation¹:

$$i = \frac{nFAC\sqrt{D}}{\sqrt{\pi t}} \quad \text{Eq. 3}$$

where i is the measured current and t is time, the D estimated for $3.23 \times 10^{-6} \text{ cm}^2 \text{ s}^{-1}$. The diffusion coefficient was averaged from the values of three different methods: $D = 3.08 \times 10^{-6} \text{ cm}^2 \text{ s}^{-1}$, with a standard deviation of $1.50 \times 10^{-7} \text{ cm}^2 \text{ s}^{-1}$.

High resolution optical images of graphene flakes

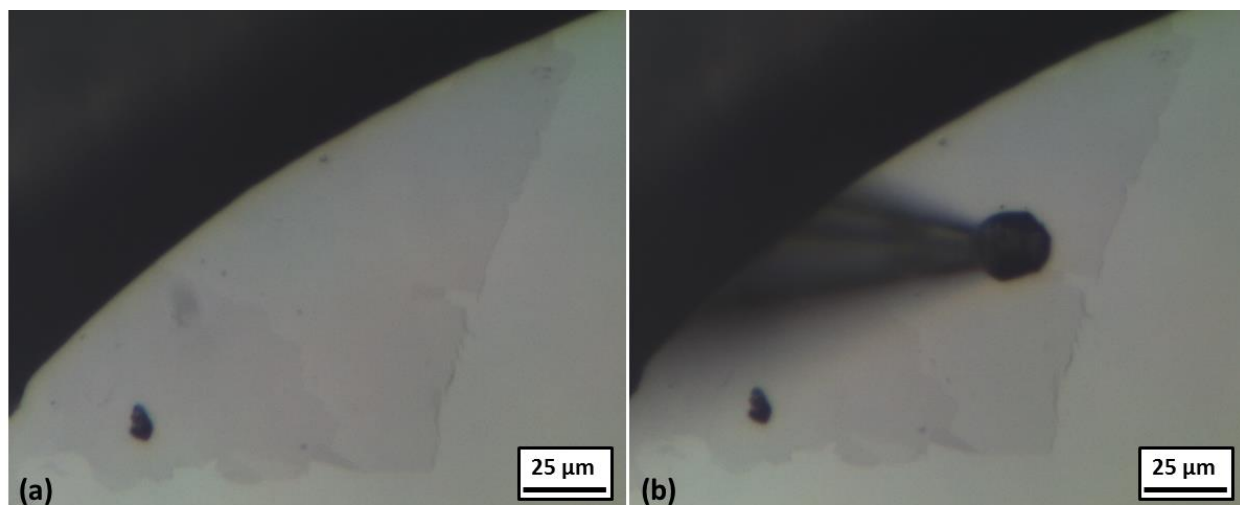


Figure S3. Optical micrographs of monolayer graphene flakes, before (a) and after (b) droplet deposition to the basal plane of monolayer (specimen A).

The optical micrographic image in Fig S3a shows a mono- and bilayer graphene flakes contacted by silver paint (black triangle in the right corner), the darker bilayer is visible in the lower part of the image. The deposited 10 μm radius aqueous droplet (specimen A) and the micropipette tip (black arrow) could be seen in Fig S3b. Figure S4a shows two darker bilayer flakes (the lower triangle and the upper trapezoidal shape) and, under them, a monolayer one. Fig S4b shows the 10 μm radius droplet on the triangle shape bilayer flake (specimen B).

The darker triangle and above trapezoidal shaped flakes clearly show the difference between the monolayer flake underneath the bilayers (Fig S4a). Similar differences could be seen in the contrast of colours on the edge/step between the mono- and bilayer flakes (Fig S3a). According to the pioneering work of Blake *et al.*² the graphene layers on the Si/SiO₂ substrate can be visualized and characterised using optical microscopy.²⁻⁴

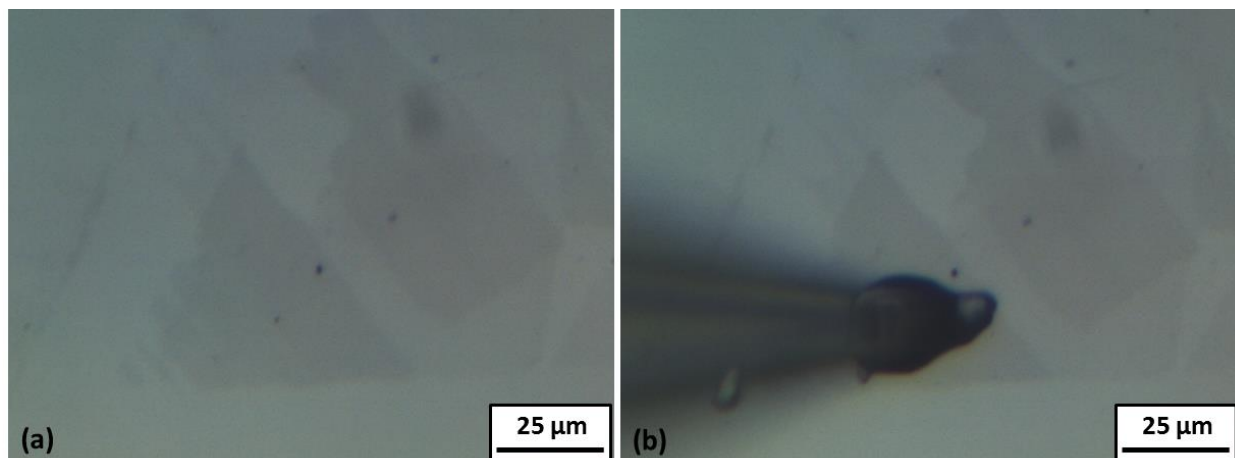


Figure S4. Optical micrographs of bilayer graphene flakes, before (a) and after (b) droplet deposition onto the basal plane of the bilayer (specimen B).

Damage of graphene on Si/SiO₂ substrate

An AFM image (Fig S5) was obtained after a deposition of 6 M LiCl aqueous electrolyte droplet on monolayer graphene at Si/SiO₂ substrate, the rupture of monolayer graphene in the centre of the image and part of the substrate in the lower right corner can be seen. The inset shows the optical micrograph of the cantilever near the injected droplet: the shapes of droplets are the same as shown in Fig 4b (in the main manuscript).

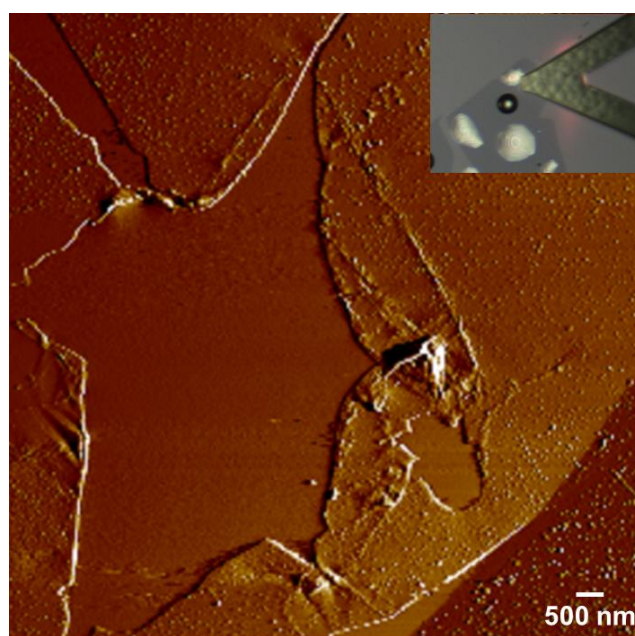


Figure S5. AFM image of the damaged monolayer graphene layer at Si/SiO₂ surface, the inset shows the cantilever on the deposited droplet, scale bar: 500 nm.

References

1. A. J. Bard and L. R. Faulkner, *Electrochemical Methods: Fundamentals and Applications*, Wiley, New York, 1980.
2. P. Blake, E. W. Hill, A. H. Castro Neto, K. S. Novoselov, D. Jiang, R. Yang, T. J. Booth and A. K. Geim, *Appl. Phys. Lett.*, 2007, **91**, 063124-1-3.
3. I. Calizo, I. Bejenari, M. Rahman, G. Liu and A. A. Balandin, *J. Appl. Phys.*, 2009, **106**, 043509-1-5.
4. R. Sharma, J. H. Baik, C. J. Perera and M. S. Strano, *Nano Lett.*, 2010, **10**, 398-405.